Coupling of rock uplift and river incision in the Namche Barwa–Gyala Peri massif, Tibet

Noah J. Finnegan[†]*
Bernard Hallet
David R. Montgomery
Department of Earth and Space Sciences and Quaternary Research Center, University of Washington, P.O. Box 351310, Seattle, Washington 98195, USA

Peter K. Zeitler
Department of Earth and Environmental Sciences, Lehigh University, 31 Williams Drive, Bethlehem, Pennsylvania 18015, USA

John O. Stone
Department of Earth and Space Sciences and Quaternary Research Center, University of Washington, P.O. Box 351310, Seattle, Washington 98195, USA

Alison M. Anders
Department of Geology, University of Illinois at Urbana-Champaign, 245 Natural History Building, 1301 West Green Street, Urbana, Illinois 61801, USA

Liu Yuping
Chengdu Institute of Geology and Mineral Resources, 2 Beisanduan, Yihuanlu, Chengdu 610081, Sichuan Province, China

ABSTRACT

Geodynamic modeling demonstrates the strong potential for erosion to influence the pattern and style of deformation in active mountain belts, but field studies yield conflicting views on the importance of erosion in influencing orogenesis. Here we compare patterns in river power, inferred excess fluvial-transport capacity, topographic relief, precipitation, and mineral-cooling ages to assess the coupling between surface erosion and rock uplift within the vicinity of the Namche Barwa–Gyala Peri massif, an active antiformal structure within the eastern Himalayan syntaxis. Our rich and dense data set reveals a tight spatial correspondence of fluvial incision potential, high relief, and young cooling ages. The spatial coincidence is most easily explained by a sustained balance between rock uplift and denudation driven by river incision over at least the last ~1 m.y. The Yarlung Tsangpo–Brahmaputra River is the largest and most powerful river in the Himalaya, and two lines of evidence point to its active role in the dynamic interaction of local erosion, rock uplift, thermal weakening of the lithosphere, and deformation: (1) Whereas along the rest of the Himalayan front, high relief and high rock uplift rates are essentially continuous, the high relief and rapid exhumation in the syntaxis is restricted to a "bull's-eye" pattern exactly where the largest river in the Himalaya, the Yarlung Tsangpo–Brahmaputra, has the most energy per unit area available to erode its channel and transport sediment. (2) The location of rapid incision on the Yarlung Tsangpo–Brahmaputra has been pinned for at least 1 m.y., and without compensatory uplift of the Namche Barwa–Gyala Peri massif during this time the river would have eroded headward rapidly, incising deeply into Tibet.

Keywords: river incision, rock uplift, climate, tectonics and landscape evolution, eastern Himalayan syntaxis, Namche Barwa.

INTRODUCTION

The potential for spatial patterns in erosion to influence the location of deformation in active mountain belts is well established in numerical models (e.g., Willett, 1999; Beaumont et al., 2001; Koons et al., 2002). Additionally, the tendency for rivers to grow steeper, convey more water, and become more erosive with higher rates of tectonic uplift is also documented in numerical models (Whipple and Tucker, 1999; Anders, 2005). Such work has led to wide acknowledgment of the idea that rates of rock uplift with respect to the geoid and rates of surface erosion should be driven toward a dynamic balance in actively uplifting ranges. Coupling between rock uplift and surface erosion, in turn, has important implications for geodynamics. This is because patterns in topography and climate, to the extent that they reveal erosion rate patterns, can provide constraints on spatial gradients in rock uplift rates, which commonly lack clear surface expression in heavily dissected and hard to access terrain (e.g., Seeber and Gornitz, 1983; Finlayson et al., 2002; Wobus et al., 2003; Kirby et al., 2003; Wobus et al., 2006). Additionally, recent models demonstrate that the width and height of active mountain ranges may be controlled by rates of erosion (Whipple and Meade, 2004; Stolar et al., 2006; Roe et al., 2006; Willett et al., 2006). Finally, coupled surface and thermo-mechanical models show that focused erosion, even on the comparatively local scale of a large river valley system, can have dramatic consequences for the deformation of crustal lithosphere, leading to localized feedbacks between erosion, deformation, and rock uplift (Koons et al., 2002).

The latter scenario, dubbed a *tectonic aneurysm,* arises from the dynamic interactions of

[†]E-mail: njf7@cornell.edu
*Present address: Department of Earth and Atmospheric Sciences, Cornell University, Snee Hall, Ithaca, New York 14853-1504, USA

GSA Bulletin; January/February 2008; v. 120; 1/2; p. 142–155; doi: 10.1130/B26224.1; 12 figures; Data Repository item 2008002.

localized erosion, topographic stresses, rock uplift, thermal weakening of the lithosphere, and deformation (Koons et al., 2002). The Nanga Parbat–Haramoosh massif in Pakistan exhibits the interconnected geomorphic, geophysical, petrologic, and geochemical evidence that initially inspired the aneurysm model (Zeitler et al., 1993, 2001a; Meltzer et al., 1998; Park and Mackie, 2000): a large, powerful, and rapidly incising river, the Indus, cuts a deep gorge adjacent to an isolated, high-relief massif marked by extremely rapid cooling, and an upwardly bowed Moho. Nanga Parbat's eastern counterpart, the Namche Barwa–Gyala Peri massif, punctuates the eastern terminus of the Himalaya Arc. The major east-flowing orogen-parallel river, the Yarlung Tsangpo–Brahmaputra, wraps around the Himalayan arc here, cutting a spectacular gorge into the easternmost high Himalaya. Field observations, analysis of coarse-scale digital-elevation data, and mineral-cooling age data suggest that the superposition of the 5-km-deep Yarlung Tsangpo gorge and the rapidly cooled and deeply incised Namche Barwa–Gyala Peri massif is consistent with local coupling between erosion and crustal deformation in this region (Burg et al., 1998; Zeitler et al., 2001b; Koons et al., 2002). However, until recently, neither the geomorphology nor the thermal history of this region has been characterized with sufficient detail to confirm such coupling with any satisfaction, and hence to begin to address the unique geodynamics of this region.

The first of the three goals of this paper, therefore, is to investigate the tectonic aneurysm hypothesis by assessing the extent of coupling between regional denudation driven by the Yarlung Tsangpo–Brahmaputra River and rock uplift within the core of the eastern Himalayan syntaxis. To this end we first review newly published biotite $^{40}Ar/^{39}Ar$ ages, zircon (U-Th)/He ages, and structural geology from the Namche Barwa–Gyala Peri massif. We next compute spatial patterns in river power to provide an index of the rate of detachment-limited fluvial incision within the field area. However, acknowledging the important dual role of sediment in both sustaining and suppressing channel incision, we also use river power and valley-bottom sediment storage, respectively, as indices of bed load transport capacity and excess transport capacity within the conceptual framework of the saltation-abrasion model of Sklar and Dietrich (2004). We compare patterns in the two indices of fluvial incision rate to patterns in mineral cooling and mapped structures to assess the accord between regional denudation driven by river incision, deformation, and exhumation over the Quaternary. We then discuss the implications of this coupling in light of geodynamic models for this region.

The second and more general goal of this paper is to provide additional insight into how sustained high erosion rates are expressed topographically and geomorphologically in active mountain belts. Despite considerable attention, there is still little consensus on which topographic metrics are likely to reflect adjustment to long-term rates of rock uplift. The Namche Barwa–Gyala Peri massif and its surroundings are ideally suited as a natural laboratory to elucidate the coupling between erosion and rock uplift in active mountain belts, because the study area is characterized by large and now well-constrained gradients in exhumation, precipitation, fluvial power, fluvial-sediment transport capacity, and topographic relief. Thus, the likelihood of discerning a signal in both exhumation and topography that is above inherent noise levels is arguably higher here than elsewhere in the Himalaya.

Finally, because the extent to which patterns in precipitation alone control patterns in exhumation remains vigorously debated (Reiners et al., 2003; Burbank et al., 2003; Wobus et al., 2003; Thiede et al., 2005), our third goal is to examine patterns in precipitation independently of patterns in river incision potential to assess their spatial relationship to apparent exhumation rate gradients. This is possible within the study area because, in contrast to the majority of other Himalayan rivers with little source area on the Tibetan Plateau, the Yarlung Tsangpo–Brahmaputra River conveys a huge volume of water from the Tibetan Plateau in comparison with the volume of locally sourced orographic precipitation within the Namche Barwa–Gyala Peri massif. Thus patterns of orographic precipitation within the massif and patterns of river power on the Yarlung Tsangpo–Brahmaputra River are effectively independent of one another and can be deconvolved and compared individually to patterns in mineral cooling to assess the relative influences of both river incision and precipitation on rock uplift.

OVERVIEW OF GEOLOGY, TECTONICS, AND GEOMORPHOLOGY

The eastern Himalayan syntaxis is the eastern termination of the great Himalayan Arc. As such, it spans the transition from dip-slip thrust tectonics along the Himalayan front to the largely strike-slip tectonics responsible for accommodating the northern motion of India relative to SW China and Myanmar (Burg et al., 1997). The syntaxis is developed over the NE corner of the indenting Indian plate and is a crustal manifestation of the complex lithospheric deformation taking place in this region of structural transition. The syntaxis is marked by a spectacular arcuate deflection around the indenting Indian plate corner of geologic units, structural fabric, topography, and global positioning system (GPS)–derived plate velocity vectors (Tapponnier et al., 1982; Royden et al., 1997; Hallet and Molnar, 2001; Zhang et al., 2004; Sol et al., 2007).

Embedded within the syntaxis is an active antiformal metamorphic structure, the Namche Barwa–Gyala Peri massif, which is composed of Precambrian Himalayan basement that has recently been undergoing active deformation and rapid unroofing, partially coeval with an anatectic episode under way for the past 10 m.y. (Burg et al., 1997; Booth et al., 2004; Malloy, 2004; Zeitler et al., 2006). Field mapping and thermochronometry indicate that the northern tip of the syntaxis is cross-cut by a major north-dipping crustal-scale shear zone and fault, the Nam-La thrust zone (Ding et al., 2001) (Fig. 1A). The Nam-La thrust bounds to the south an antiformal crustal pop-up (Burg et al., 1997) that contains the two highest peaks for several hundreds of kilometers along the Himalaya: the 7782 m Namche Barwa and the 7294 m Gyala Peri. Cooling ages drop to the north across this inferred structure, indicating that the Namche Barwa–Gyala Peri antiform has been recently and rapidly exhumed relative to the surrounding terrain (Burg et al., 1997; Malloy, 2004; Zeitler at al., 2006). The antiform itself is complexly folded but shows fabrics and fold axes consistent with N-S to NW-SE compression (Burg et al., 1998; Ding et al., 2001; Kidd et al., 2006).

Just to its north the Namche Barwa–Gyala Peri antiform is flanked by the Jiali Fault Zone, a SE-NW–oriented dextral strike-slip fault that accommodates clockwise crustal rotation around the syntaxis (Armijo et al., 1989; Burg et al., 1998). Recent activity on the fault is evident in much of the topography in the vicinity of the syntaxis (Figs. 1A–1B); however, slip rates are unconstrained, and the presence of the fault is inferred on the basis of its topographic expression and the juxtaposition of differing lithologies along its trace.

An interesting topographic consequence of an indenting plate corner is that it will tend to entrain major orogen-parallel rivers that have been forced to flow behind the mountain front as peaks have uplifted (Koons, 1995; Zeitler et al., 2001b). On a much smaller scale, this is analogous to a river being diverted by a growing anticline and forced to flow around its tip. In the case of the eastern syntaxis, the Yarlung Tsangpo–Brahmaputra turns to the south at and through the Namche Barwa–Gyala Peri massif after flowing east for >1200 km across the southern part of the Tibetan Plateau and along the backside of the High Himalaya. It is worth noting that in the complex

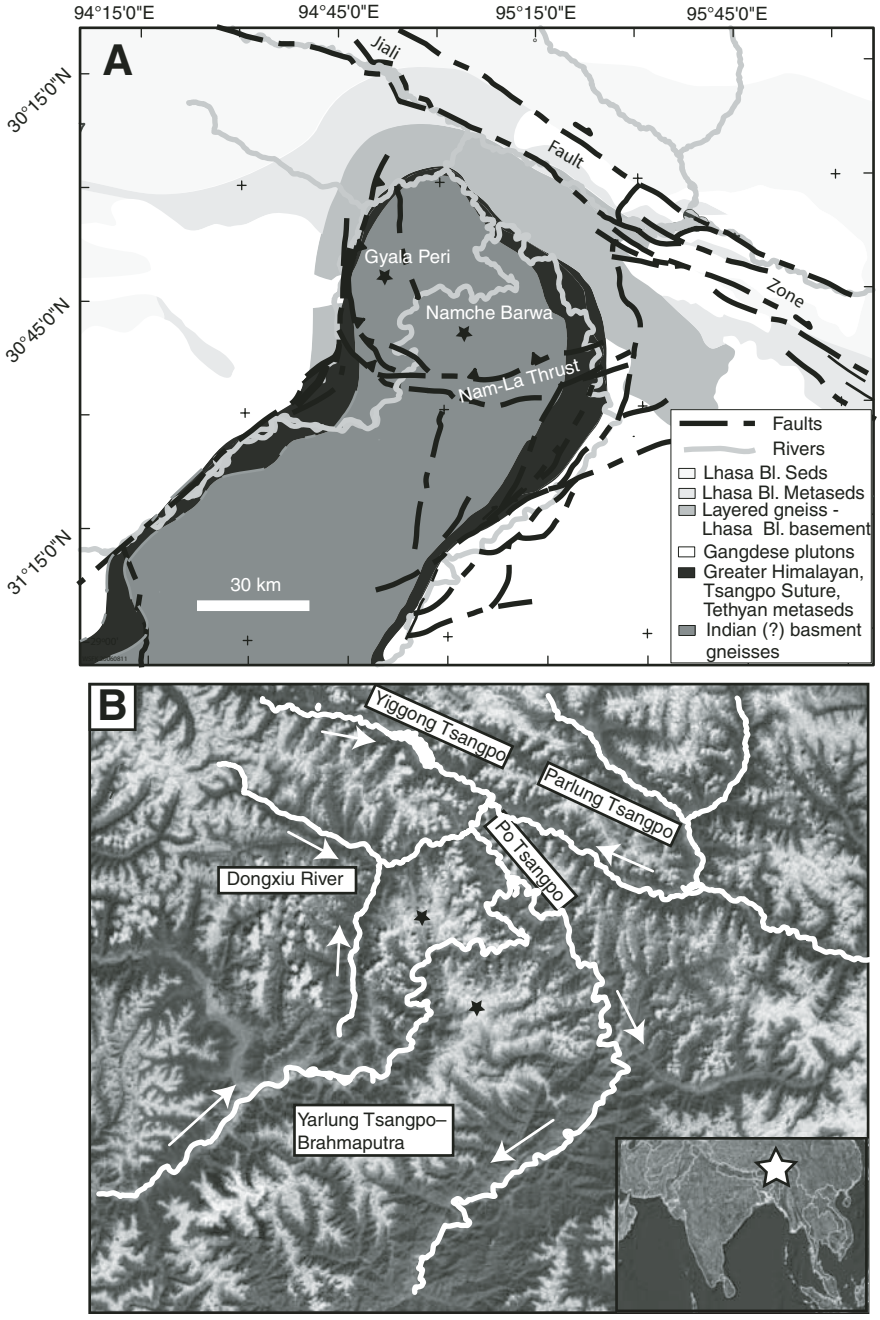

Figure 1. (A) Geologic and tectonic map of the eastern syntaxis (Burg et al., 1997, 1998; Ding et al., 2001; Kidd et al., 2006). (B) LANDSAT-7 Satellite overview of the map region in (A), highlighting major rivers. Arrows indicate river flow directions.

evolution of the region, it is also possible that an ancestral Yarlung Tsangpo–Brahmaputra River initially flowed to the southeast and out through the Irrawaddy, Parlung, or Lhuit drainage, and was captured at the syntaxis (Brookfield, 1998; Koons, 1995; Zeitler et al., 2001b; Clark et al., 2004). In either case the end result is the same, which is that the largest river in the Himalaya is now slicing through the highly deformed region at the core of the syntaxis.

Where the Nam-La thrust crosses the Yarlung Tsangpo–Brahmaputra, the river steepens and accelerates, abruptly transitioning from a sand-bedded to a boulder-strewn channel. Approximately 30 km downstream of the Nam-La thrust the river undergoes a second abrupt transition, entering a narrow bedrock gorge centered between the summits of Namche Barwa and Gyala Peri. Here, the river begins its drop from the Tibetan Plateau, descending >2 vertical km in <100 river km over one of the most spectacular knickpoints in the world.

The spatial coincidence of the Yarlung Tsangpo gorge and the Namche Barwa–Gyala Peri antiform initially led Burg et al. (1997) to suggest that regional denudation driven by the incision of the Yarlung Tsangpo–Brahmaputra passively paced rock uplift associated with an E-W–trending crustal-scale buckle fold (also recognized by Ding et al., 2001) within the syntaxis, thereby enabling nearly 30 km of rock uplift and exhumation since the late Miocene (Burg et al., 1997). More recently, Zeitler et al. (2001b) and Koons et al. (2002) suggested that instead of passively accommodating rock uplift within the antiform, denudation driven by the Yarlung Tsangpo–Brahmaputra has localized and perhaps even triggered the rock uplift of the Namche Barwa–Gyala Peri antiform.

The physical mechanism by which a river can trigger rock uplift in an orogen is provided by the tectonic aneurysm hypothesis (Zeitler et al., 2001b; Koons et al., 2002). According to the aneurysm hypothesis, focused incision by a large river, provided that tributary channels and hillslopes remain coupled to the incision of the main trunk stream, will create a rapidly eroded valley or valley system that simultaneously focuses topographic stresses and increases tectonic stresses because of the preferential removal of crustal cross-section area within the zone of rapid denudation. Where the crust is already near compressive failure, these effects may yield localized deformation and brittle failure within the valley. Thrusting, combined with continued erosion, brings hot rocks toward the surface. The advection of heat toward the surface with exhumed rocks has the effect, in turn, of dramatically reducing the integrated strength of the crust, thereby further encouraging deformation in the initial locus of erosional exhumation (Koons et al., 2002). Importantly, without changing the far-field tectonic stresses, strain rates within the impacted region increase owing to thermal weakening and localization of deformation. From a frame of reference attached to the Earth's surface, this is manifested in increasing rates of rock uplift with respect to the surface (Koons et al., 2002). Therefore high topography and relief related to increasing vertical rock-uplift rates will develop in association with the initial excavation of the river valley. In this way, isolated topographic massifs with high relief and rapid cooling can paradoxically owe their existence to river incision. Although the importance of erosion is widely acknowledged at the orogen scale (e.g., Willett, 1999), what distinguishes the tectonic aneurysm hypothesis is that it suggests a physical mechanism for a much more localized coupling between erosion and rock deformation.

CONSTRAINTS AND OBSERVATIONS

He and Ar Thermochronometry

Malloy (2004) and Zeitler et al. (2006) reported an extensive suite of (U-Th)/He and $^{40}Ar/^{39}Ar$ cooling ages for apatite, zircon, and biotite from terranes in SE Tibet, with many of their data coming from within and near to the Namche Barwa–Gyala Peri massif. Most directly, such ages reflect the thermal histories of their host rock. In a region like SE Tibet that has been subjected to repeated structural events and that is marked by rugged and possibly changing topography, attempts to convert cooling information into exhumation rates will be complicated by the evolving thermal field (e.g., Stuwe et al., 1994). Therefore, following Zeitler et al. (2006), we interpret their reported ages as cooling ages, treating patterns in these ages as proxies for patterns in relative exhumation rates. In particular, we use (U-Th)/He zircon ages to determine the time since a sample cooled from 185–210 °C (Reiners et al., 2002), and $^{40}Ar/^{39}Ar$ biotite ages to record the time since a mineral cooled from 300–335 °C (Grove and Harrison, 1996). In order to illustrate gradients in exhumation in the field area, we have highlighted young cooling ages in the study area in Figures 2 and 3.

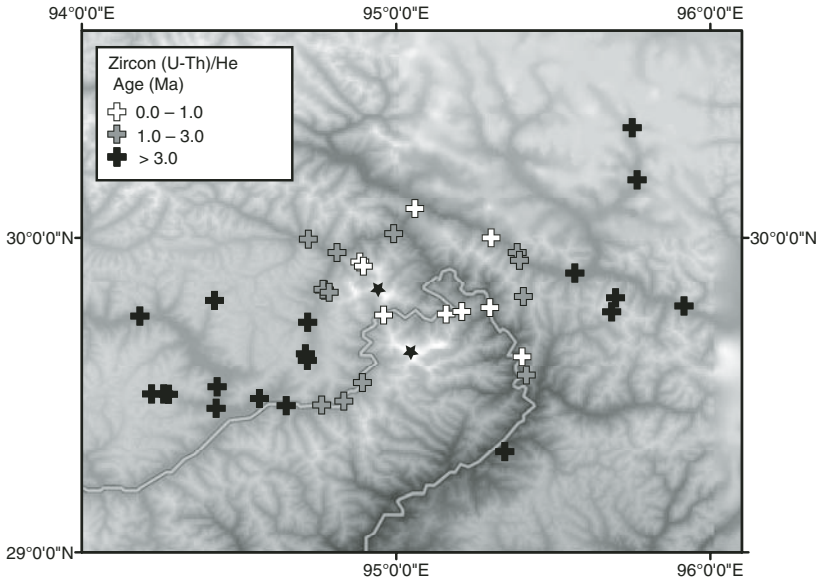

Figure 2. Spatial distribution of zircon (U-Th)/He ages in the vicinity of the Namche Barwa–Gyala Peri massif. Stars denote the locations of Namche Barwa and Gyala Peri.

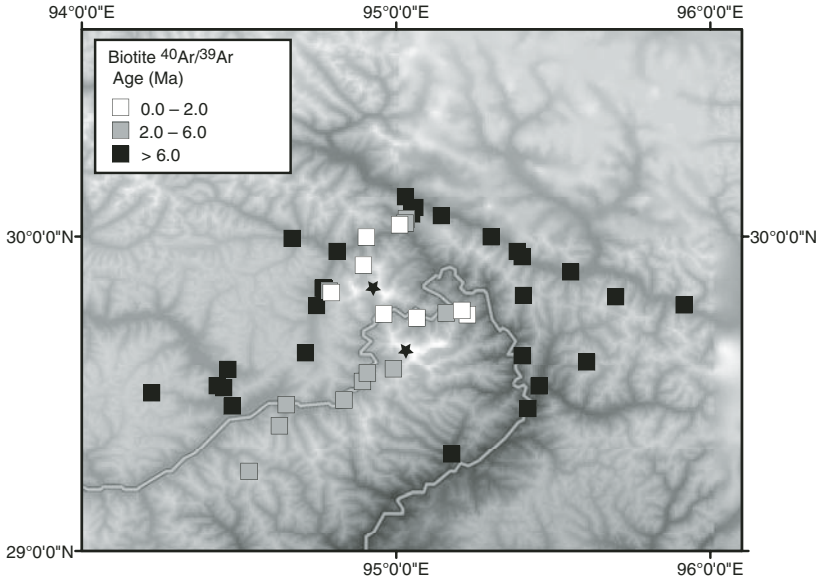

Figure 3. Spatial distribution of biotite $^{40}Ar/^{39}Ar$ ages in the vicinity of the Namche Barwa–Gyala Peri massif. Stars denote the locations of Namche Barwa and Gyala Peri.

The mineral-cooling data reveal a prominent "bull's-eye" pattern of young ages confined to the Namche Barwa–Gyala Peri massif and its immediate vicinity that is expressed in the higher-temperature data sets, (U-Th)/He zircon and $^{40}Ar/^{39}Ar$ biotite, reported in Malloy (2004) and Zeitler et al. (2006) (Figs. 2 and 3). However, important differences between the patterns are revealed by the two data sets. Young biotite ages (0.9–2 Ma) are contained within the mapped, bounding structures of the Namche Barwa–Gyala Peri massif. In contrast, extremely young zircon helium ages (0.3–1 Ma) extend across terranes and structures, expanding the region of apparently rapid exhumation into the lower Parlung River watershed, in comparison with the pattern of $^{40}Ar/^{39}Ar$ cooling ages. Zeitler et al. (2006) suggest that this pattern is most likely to reflect the recent acceleration of erosion owing to the northward propagation of the north-plunging Namche Barwa–Gyala Peri antiform, and that overall the thermochronometric data provide evidence for considerable and rapid exhumation of the antiform relative to its surroundings since 5 Ma or earlier.

Topographic Relief and Basin-Averaged Erosion Rates

Rock uplift drives relief production in active orogens, and in the Himalaya high relief is associated with high rock-uplift rates (e.g., Seeber and Gornitz, 1983; Lavé and Avouac, 2001; Bendick and Bilham, 2001). A relationship between relief and erosion rate, in turn, is expected in active orogens where rates of slope-dependent surface erosion and rock uplift have had sufficient time to equilibrate, such as is likely for the Himalaya, where convergence has been ongoing for 50 m.y. (e.g., Hodges, 2000). In the vicinity of the Namche Barwa–Gyala Peri antiform, ^{10}Be-derived erosion rates in river sediments clearly increase ($R^2 = 0.81$ for power law fit) with topographic relief and mean basin slope (Table DR1[1]). This trend, corrected for

[1]GSA Data Repository Item 2008002, details related to river power calculations and ^{10}Be analysis, is available at www.geosociety.org/pubs/ft2007.htm. Requests may also be sent to editing@geosociety.org.

the effects of snow and ice cover, holds over an order of magnitude of erosion rates (0.1–4 mm/yr) and over a 3000 m range of mean relief. The trend is also consistent with ^{10}Be-derived catchment erosion rates from the western Himalaya and various erosion rate measurements elsewhere indicating that the erosion rate increases nonlinearly with relief (Vance et al., 2003; Montgomery and Brandon, 2002).

We note that numerical modeling (Niemi et al., 2005) demonstrates that ^{10}Be erosion rate estimates for small-order, landslide-dominated catchments, such as we sampled along the Parlung River, will tend to systematically underestimate basin-averaged erosion rates because large and infrequent landslides dominate the erosion of these catchments, but typically these are not sampled. Our data (Table DR1; see footnote 1), however, indicate that the small first and second order catchments draining into the Parlung River exhibit uniformly higher erosion rates, 1.9 ± 0.39 to 3.57 ± 0.74 mm/yr, than the Parlung Basin as a whole, 1.07 ± 0.22 mm/yr, or than any of the larger catchments sampled, with the exception of NB-4–04. This is most likely due to the fact that the smaller basins sampled in our analysis are much steeper on average than the larger basins. Hence, although drainage basin size may influence our ^{10}Be erosion rate estimates, it appears that this effect is secondary to the much larger influence that relief variation has on basin-averaged erosion rates within the study area.

In Figure 4A we plot regional patterns in relief, calculated as the maximum range in elevation within a ~10 km radius circle for each pixel in the GTOPO 30 digital elevation data set. Figure 4B, in turn, shows the close correspondence between areas of rapid erosion inferred from ^{10}Be analyses, and areas of high relief. For this figure, relief was computed at each point in the watershed (again as the maximum range in elevation within a ~10 km radius circle for each pixel in the watershed), and then these points were averaged for the entire watershed to yield a single basin-averaged relief value. Taken together, Figures 4A and 4B show, much the same as the pattern in cooling ages, a "bull's-eye" of high relief and high inferred erosion rates centered on the Namche Barwa–Gyala Peri massif.

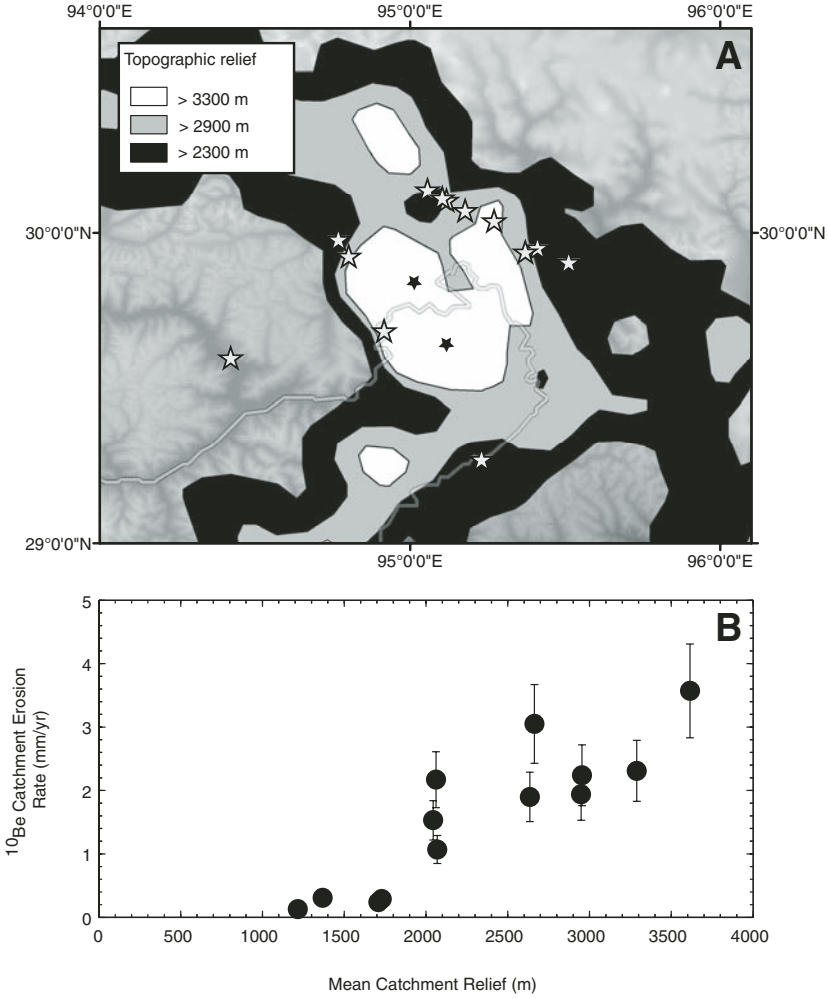

Figure 4. (A) Patterns in topographic relief in the vicinity of the Namche Barwa–Gyala Peri massif. Areas with no data coverage are those with relief <2300 m. Gray stars denote the locations of sediment samples taken for ^{10}Be analysis. Black stars show the locations of Namche Barwa and Gyala Peri. (B) ^{10}Be basin-averaged erosion rate vs. mean topographic relief for sampled catchments.

Precipitation

For the Himalaya the extent to which orographic precipitation patterns directly influence patterns in long-term exhumation rates is debated. Although it is speculated that orographic precipitation patterns are important to the geodynamics of the Himalayan front (Beaumont et al., 2001; Wobus et al., 2003), actual comparisons of patterns of precipitation and exhumation rates along the Himalaya yield conflicting views of the apparent influence of precipitation alone on rock uplift (Burbank et al., 2003; Thiede et al., 2005). To further explore the role of precipitation in influencing exhumation within and around the Namche Barwa–Gyala Peri massif, we define precipitation patterns with the TRMM (Tropical Rainfall Measuring Mission) satellite. As described in the next section, we also use the TRMM satellite data to generate river discharges that incorporate observed spatial patterns in precipitation, as well the drainage basin architecture of the study area.

Using the TRMM-derived rainfall data set compiled by Anders et al. (2006) for the period 1998–2001, we are able to define mean annual precipitation for the study area at a resolution of ~10 km × 10 km. As discussed by Anders et al. (2006), this spatial resolution reflects an optimization of grid resolution and temporal sampling density. At the ~10 km × 10 km resolution, each pixel records between ~2856 and ~12,696 individual instantaneous rain rate measurements over the period 1998–2001, from which the mean annual precipitation rates shown in Figure 5 are computed. The gross pattern of precipitation in the field area is closely related to the topography of the syntaxis (Anders et al., 2006). The lower Yarlung Tsangpo–Brahmaputra Valley appears to funnel moisture up-valley to the first major northward bend in the river, at which point precipitation falls off steeply to <1 m/yr. Heavy precipitation therefore appears restricted to the region to the south and downstream of the high

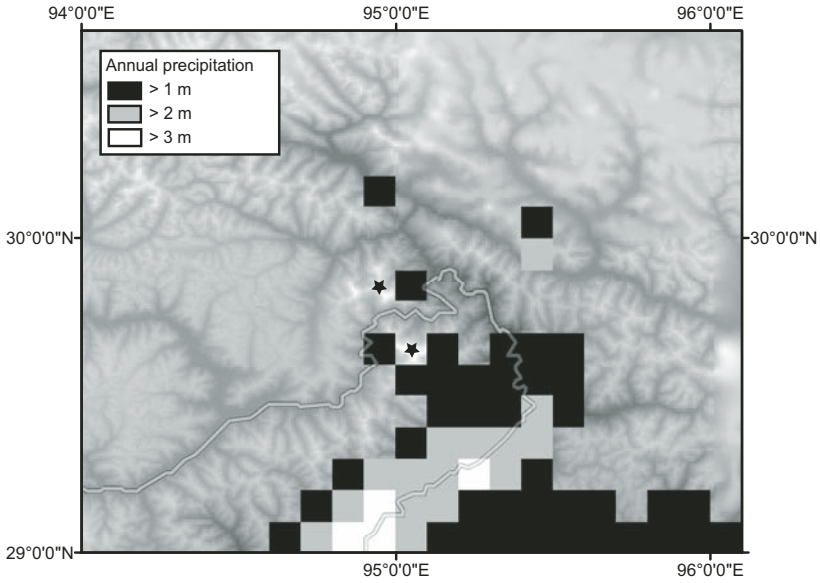

Figure 5. Patterns in mean annual precipitation in the vicinity of the Namche Barwa–Gyala Peri massif. Areas with no data coverage are those with <1 m of precipitation annually. Stars denote the locations of Namche Barwa and Gyala Peri.

topography of the Namche Barwa–Gyala Peri massif. Importantly, the TRMM data indicate that heavy rainfall does not penetrate the rapidly cooled Namche Barwa-Gyala Peri massif.

RIVER INCISION

The detachment-limited stream power model (Howard, 1994) provides an index of the rate of fluvial incision where the mechanism of incision scales with the magnitude of mean bed shear stress or stream power, such as is expected where erosion is dominantly due to the plucking of jointed bedrock (Whipple et al., 2000). Although this family of models overlooks a number of important characteristics of mountain channels (e.g., Stock and Montgomery, 1999; Sklar and Dietrich, 2001; Sklar and Dietrich, 2004; Molnar et al., 2006), stream power and shear stress models have nevertheless been validated in many settings (e.g., Stock and Montgomery, 1999; Kirby and Whipple, 2001; Lavé and Avouac, 2001; Wobus et al., 2003).

Commonly, stream power or shear stress approaches assume that the variables that are key to incision scale in a simple way with either slope or drainage area, and then via a series of further assumptions and substitutions (e.g., Whipple and Tucker, 1999) cast incision as a function of quantities that can be obtained from a digital elevation model (DEM). In this way, spatial patterns in incision rates can be inferred over broad geographic domains (e.g., Finlayson et al., 2002; Wobus et al., 2003). Wide acknowledgment of the importance of orographic precipitation gradients (Lavé and Avouac, 2001; Roe et al., 2002) and channel width variation (e.g., Lavé and Avouac, 2001; Montgomery and Gran, 2001) in modifying spatial patterns in stream power or shear stress has led to more refined approaches to inferring spatial incision-rate patterns (e.g., Lavé and Avouac, 2001; Finnegan et al., 2005; Whittaker et al., 2007). In keeping with these approaches, we compute spatial patterns in river power for the large rivers within the syntaxis using direct measurements of channel width and TRMM satellite-derived river discharges, in addition to measurements of channel slope determined from digital elevation data. The combination of TRMM data and channel width measurements allows us to compute river power in a manner that incorporates pronounced orographic precipitation patterns (Fig. 5), and the rich variation in channel width observed within the vicinity of the Namche Barwa–Gyala Peri massif (Finnegan et al., 2005).

We calculate mean annual river power for the Yarlung Tsangpo–Brahmaputra and its major tributaries in the vicinity of the Namche Barwa–Gyala Peri massif as follows:

$$\Omega = \rho g Q S / W, \quad (1)$$

where ρ is the density of water, g is the acceleration due to gravity, Q is mean annual river discharge, S is channel slope, and W is channel width.

We obtain estimates of mean annual river discharge throughout the field area by routing annually accumulated TRMM satellite-derived rainfall on the 30 arc-second GTOPO 30 DEM of Asia. Anders et al. (2006) show that estimates of river discharge using TRMM data systematically under-predict gauged mean annual discharges for 21 Himalayan catchments, probably owing to the fact that TRMM's relatively infrequent sampling interval does not capture all precipitation events. Anders et al. (2006) calculate, specifically, that TRMM-derived annual river-discharge measurements are on average 22% lower than gauged discharges. We therefore apply a correction to the TRMM-derived river discharges to compensate for the systematic underprediction by TRMM of actual mean annual discharges.

Channel slopes and elevation profiles for the Jiggong Tsangpo, Yarlung Tsangpo–Brahmaputra, and most of the Parlung Tsangpo were calculated from the 3 arc-second (~90 m) Defense Mapping Agency Digital Terrain Elevation Data (DTED) for Asia. Because of the inherent noise in digital elevation data, we averaged river elevation data by 10 km reaches in order to obtain smooth and statistically significant river elevation profiles and channel slopes. The vertical accuracy of the 3 arc-second data is estimated to be ±18 m (U.S. Geological Survey, 1993). However, as we have averaged the 90 m resolution data into 10 km reaches, the standard error of the mean elevation for each elevation bin becomes ±1.7 m. We calculate channel slope, in turn, by computing the centered difference elevation gradient using the elevation points directly upstream and downstream of the point of interest. Hence, over this 20-km-length scale, errors in mean channel slope can be expected to be as high as 3.4 m out of 20,000 m, or ~0.02% when 3 arc-second elevation data are averaged over 10 km reaches, as we have done.

Three arc-second DTED data were unavailable for the Po Tsangpo, the lower Parlung, and the Dongxiu river system, whereas 3 arc-second SRTM topographic data are for the most part unusable in the field area owing to widespread data dropouts there. We therefore use the GTOPO30 30 arc-second DEM (http://edc.usgs.gov/products/elevation/gtopo30/gtopo30.html) to determine river slopes for these rivers, again by averaging the elevation data into 10 km reaches to smooth noise in the data. Most of Eurasia in the GTOPO30 data set is simply a resampled version of the DTED 3 arc-second data (http://edc.usgs.gov/products/elevation/gtopo30/gtopo30.html), which, as mentioned above, has a nominal vertical accuracy of ±18 m. Assigning this same vertical accuracy to the GTOPO30 derived data, we therefore compute that for elevation averaged over a 10 km reach the standard elevation error will be ±5.7 m. Again, using a centered difference slope

computation, this means that errors in slope will be as high as 11.4 m out of 20,000 m, or 0.06%. We emphasize that although these may initially seem like optimistic error evaluations, they apply only to the data averaged over 10 km.

Additional uncertainty in estimating river longitudinal-profile slopes is also introduced where DEM grid resolution is much larger than river channel width, as is almost always the case for GTOPO30. In this case, the fine-scale structure of rivers, such as meandering, is lost, and pixels identified via geographic information system (GIS) flow accumulation algorithms as "river" pixels may actually average in substantial parts of adjacent hillslope elevations. Consequently, local channel elevation may be overestimated on the basis of the amount of hillslope elevation included in a given grid cell, whereas flow length can be underestimated because of the degree to which meandering is not represented in the DEM. The combination of these errors produces additional uncertainty in channel slope calculations that are not included in the accuracy estimates discussed above.

In order to assess the uncertainty introduced into our slope estimates owing to the coarse resolution of the 30 arc-second GTOPO30 DEM, we directly compare channel slope for the Yarlung Tsangpo–Brahmaputra computed from the GTOPO30 30 arc-second DEM averaged over 10 km to channel slope computed from the DTED 3 arc-second DEM averaged over 10 km. This comparison is shown in detail in Figures DR1A and DR1B (see footnote 1). However, to summarize, channel slopes computed from GTOPO30 are on average 12% ± 8% higher than channel slopes computed from the DTED 3 arc-second data for the Yarlung Tsangpo–Brahmaputra. This is because the GTOPO30 data set, as discussed above, neglects some of the meandering in the channel that is captured by the DTED data, yielding a flow length difference of ~2.5% over the 400 km of the river addressed in this study. To compensate for this systematic overestimation of channel slope by GTOPO30, we apply a correction to all slope measurements estimated from GTOPO30 data.

There is also considerable scatter in the plot of DTED slope versus GTOPO30 slope (Fig. DR1A; see footnote 1), from which we compute a standard error in slope of 0.0033 for the GTOPO30 data averaged over 10 km. This means that beyond the 0.0006 slope uncertainty inherent in the spatially averaged GTOPO30 data, there is an additional 0.0033 uncertainty resulting from the sampling issues discussed above. Therefore, slope estimates for the Po Tsangpo, the lower Parlung, and the Dongxiu river system are known only to within 0.004 at best. We did not expand the analysis to any rivers smaller than the Po Tsangpo, lower Parlung, and Dongxiu Rivers because for smaller, lower-order channels the grid resolution of the GTOPO30 DEM approached the size of individual valleys.

We measured channel width for all of the rivers in the analysis directly from satellite imagery. For the Yarlung Tsangpo–Brahmaputra, Jiggong Tsangpo, and Parlung Tsangpo, channel width was sampled every 100 m from a continuous map of channel width created by digitizing channels from 28.5 m pixel resolution LANDSAT 7 images of the rivers at high flow, thereby providing an estimate of bankfull width. Like elevation, these width values were then averaged over 10 km to obtain a reach-mean channel width. For the Po Tsangpo, lower Parlung, and Dongxiu river system, we measured channel width directly from Google Earth (earth.google.com/) for every 1 km of channel. A reach-averaged channel width was then obtained by averaging these measurements over 10 km. Because the pixel resolution of the LANDSAT imagery for all of the measurements of width is 28.5 m, channel widths are known to, at best, within 1 pixel. Therefore we assign an uncertainty in these measurements of ±28.5 m.

To compute mean annual river power across the study region, we assume a liberal discharge uncertainty of ±20% and propagate this along with the previously discussed uncertainties in channel width and slope into the calculated values of river power. Channel slope, width, discharge, and power data are presented in Table DR2 (see footnote 1). Figure 6 illustrates the spatial pattern in river power in the vicinity of the Namche Barwa–Gyala Peri massif. Overall, mean annual river power varies from <10 W/m^2 outside of the Namche Barwa–Gyala Peri massif to a maximum of ~4000 W/m^2 in the heart of the Yarlung Tsangpo gorge. The analysis shows that high river power is centered in the region of the high topography and extreme relief within the Namche Barwa–Gyala Peri massif. The reaches of high power along the Yarlung Tsangpo–Brahmaputra and the Po Tsangpo together dissect the rapidly cooled Namche Barwa–Gyala Peri massif.

An alternative conceptual framework for modeling the rate of bedrock channel incision is provided by the saltation-abrasion model proposed by Sklar and Dietrich (2004), which provides an explicit treatment of the influence of bed load sediment supply and transport on river incision, as described below. Where bed load abrasion is the dominant incision mechanism, coarse sediment carried by rivers—depending on sediment supply relative to transport capacity—can either promote incision by providing tools or inhibit incision when deposited as a protective alluvial cover (Gilbert, 1877; Sklar and Dietrich, 1998). The Sklar and Dietrich saltation-abrasion model incorporates this fundamental nonlinearity imposed on incision by sediment dynamics.

As formulated, the saltation-abrasion model requires, at a minimum, direct constraints on both sediment supply and transport capacity integrated over a time scale of significance to the process of bedrock channel incision (i.e., centuries to

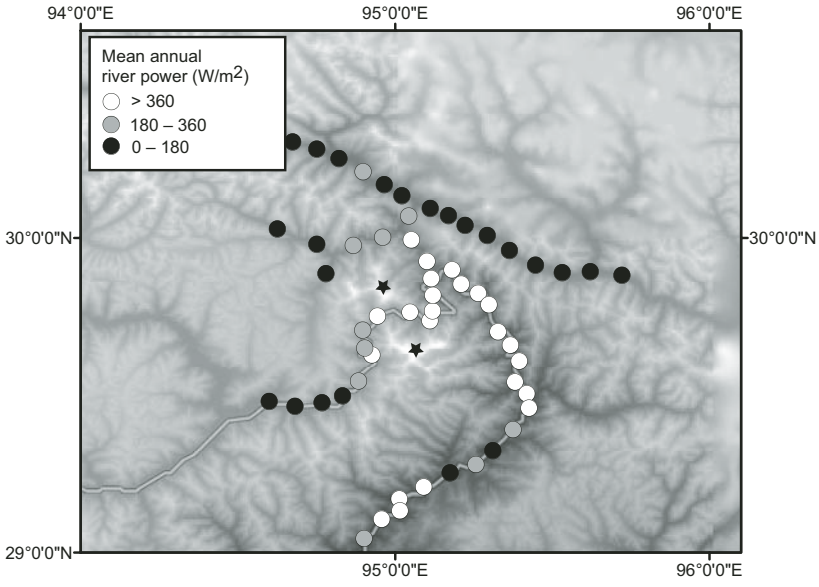

Figure 6. Patterns in mean annual river power in the vicinity of the Namche Barwa–Gyala Peri massif. Areas with no data coverage were not included in the analysis. Stars denote the locations of Namche Barwa and Gyala Peri.

millennia). Although we lack direct constraints on bed load supply within the study area, we suggest that the spatial extent of sediment terraces and deposits in valley bottoms in the vicinity of the Namche Barwa–Gyala Peri massif delineates regions of the channel network with little or no excess transport capacity, and where sediment supply is near or above the intrinsic capacity of the channel to convey it. This inference is justified by the fact that long-term storage of sediment, fundamentally, reflects sediment supply rates that exceed transport rates. For this reason, we argue that the distribution of incised alluvial terraces and currently braided channel reaches provides a proxy for supply relative to transport capacity integrated over the recent geologic past. Figure 7 depicts the spatial pattern of valley bottom deposits throughout the region of the Namche Barwa–Gyala Peri massif. The striking pattern of deposition indicates that the heart of the massif lacks long-term sediment storage altogether, whereas its distal regions appear far less capable of evacuating sediment supplied from upstream. We note that in the Yarlung Tsangpo gorge, significant sediment deposition is absent despite numerous glaciers feeding into the river, and documented peaks in regional rates of bedrock landsliding here (Bunn et al., 2004).

Just as the presence of valley-bottom alluvial deposits provides an index of low excess transport capacity channels, we further argue that the absence of alluvial deposits provides an index of channels with relatively higher excess transport capacity. In these reaches, alluvial deposition following spikes in sediment supply owing to, for instance, glacial advances or landslides, is apparently suppressed by high sediment-transport capacities.

Within the framework of the saltation-abrasion model, patterns in river power, in turn, provide an index not of incision rate but rather of bed load transport capacity. Thus comparison of Figures 6 and 7 reveals that areas of high sediment-transport capacity (i.e., power) within the Namche Barwa–Gyala Peri massif are generally spatially coincident with reaches of high excess transport capacity, whereas reaches of low and intermediate power are associated with extensive sedimentation and incised alluvial terraces, both indicative of low excess transport capacity.

Insight into relative rates of bedrock incision emerges via recognition of the fundamentally different dynamics of channels that are at or near transport capacity in comparison with those that are well below transport capacity, such as is apparently the case in the heart of the Yarlung Tsangpo gorge. Channels with low excess transport capacity, Sklar and Dietrich (2004) argue, will have incision rates that are fundamentally limited by the extent of alluvial cover deposited on the bed. Hence, positive perturbations in sediment supply in these channels will drive further sediment deposition and erosional shutdown. For example, a landslide delivered to a channel that is already at its sediment-transport capacity will lead to rapid deposition of alluvial cover and suppression of channel incision. In such an example, continued relative base-level fall and channel steepening or climate-driven changes in sediment supply or transport capacity may provide the only means for a channel to erode through protective alluvial cover and begin incising its bed again. An example of a transition to cover-limited behavior is apparent in the before and after images from a landslide delivered to the Yiggong Tsangpo in 2000 that triggered extensive alluvial deposition (Fig. 8). The images, which bracket the event in time, show the total inundation of the formerly narrow

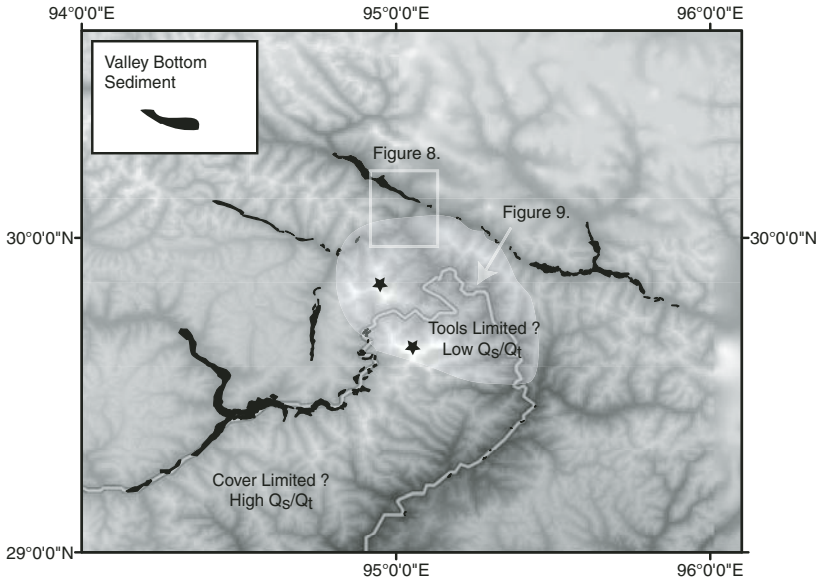

Figure 7. Valley Bottom Sediment storage in the vicinity of the Namche Barwa–Gyala Peri massif, a proxy for low excess transport-capacity channels. The locations of the reaches shown in Figures 8 and 9 are indicated in the figure. Stars denote the locations of Namche Barwa and Gyala Peri. Q_s/Q_t refers to the ratio of bed load sediment supply to bed load sediment transport capacity.

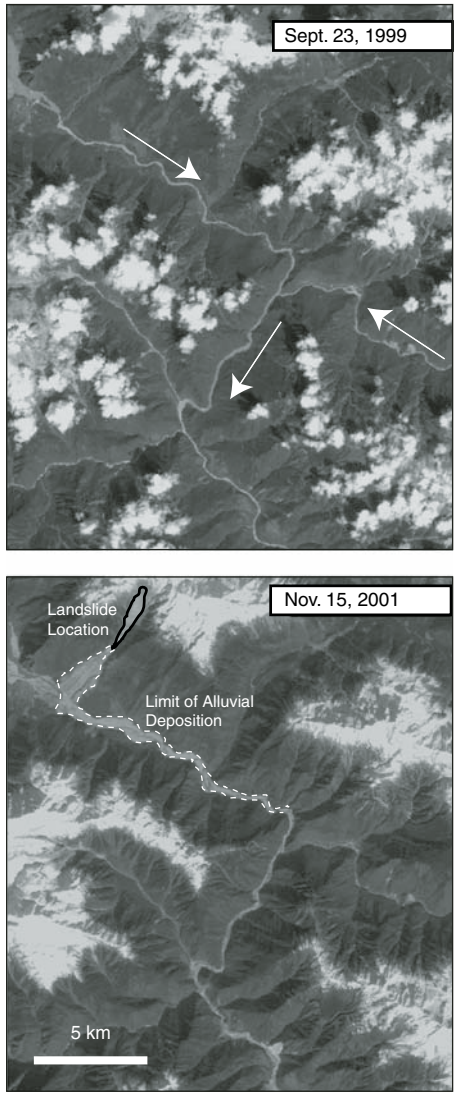

Figure 8. Paired LANDSAT images, showing the Yiggong Tsangpo before (September 23, 1999) and after (November 15, 2001) a landslide, which occurred in 2000. Arrows denote the flow directions of major rivers.

channel with a thick blanket of alluvial cover delivered from the landslide.

In contrast, based on both the saltation-abrasion model (Sklar and Dietrich, 2004) and on observations from bedrock incision experiments (Sklar and Dietrich, 2001; Finnegan et al., 2007), channels with relatively greater excess transport capacity will tend to have incision rates that are limited by the availability of erosive tools rather than the extent of alluvial cover deposition. Hence in the tools-limited regime, an excess transport capacity channel may undergo enhanced incision when supplied with landslide debris. Figure 9 shows a reach of the Yarlung Tsangpo–Brahmaputra River within the Yarlung Tsangpo gorge. Note that despite numerous large bedrock-landslide scars in the photo, sediment storage is minimal within the channel and valley bottom, confirming that the channel is capable of evacuating supplied landslide debris, and suggesting tools-limited behavior.

Importantly, whereas low excess transport-capacity channels can undergo a virtual shutdown of erosion from an influx of sediment, high excess transport channels may be able to sustain incision indefinitely, even if provided with a high supply of sediment. Thus, in regions of extensive bedrock landsliding, low excess transport-capacity channels are likely to be unstable over geologic time, oscillating between periods of alluvial deposition and renewed incision resulting from ongoing base-level fall. This effect will also be reinforced by the fact that alluvial channels are typically wider and therefore less powerful than bedrock channels for the same slope and discharge (Finnegan et al., 2005), suggesting that channels may become less capable of transport following sediment deposition.

Although landsliding and high sediment supply rates (Fig. 4) are prevalent throughout the study area, we argue that the effects of landslides will tend to amplify river incision in the Yarlung Tsangpo gorge, whereas landslide debris will retard channel incision in the regions with lower river power. Thus the regions of high power and excess transport capacity shown in Figures 6 and 7 will incise efficiently over geologic time in comparison with regions of low power and low excess transport capacity.

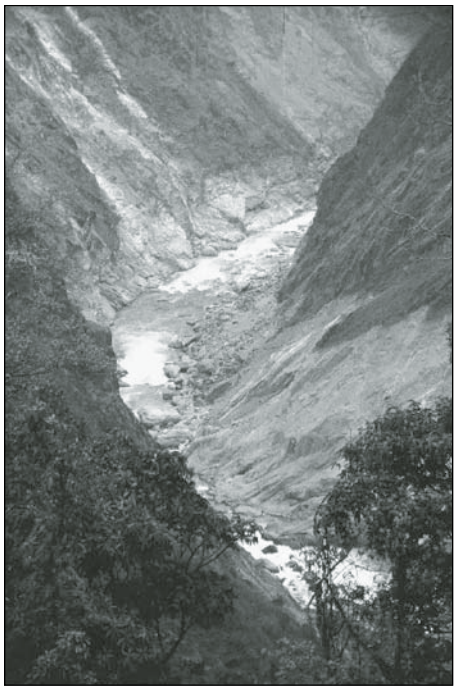

Figure 9. Photograph of the Yarlung Tsangpo–Brahmaputra within the Yarlung Tsangpo gorge, showing numerous large bedrock landslide scars and minimal sediment storage in the channel. The photograph was generously provided by Allan Ellard, a member of the 2002 kayaking expedition in the Yarlung Tsangpo gorge.

DISCUSSION

Evidence for Coupling of River Incision and Rock Uplift

Taken together, the patterns in zircon (U-Th)/He ages, biotite $^{40}Ar/^{39}Ar$ ages, topography, and river morphology reflect a striking spatial coincidence of (1) extreme topographic relief, (2) high river incision potential, (3) high fluvial bed load transport capacity relative to supply, and (4) rapid cooling centered on the Namche Barwa–Gyala Peri massif (Fig. 10). Because of this close spatial association of patterns in relief, mineral cooling, sediment-transport capacity, and river incision potential determined independently in two ways, we infer that the exhumation of the Namche Barwa–Gyala Peri massif is driven by the incision and efficient sediment transport of the Yarlung Tsangpo–Brahmaputra and the Po Tsangpo. The oversteepened slopes and pervasive bedrock landsliding within the gorge (Bunn et al., 2004) provide additional independent evidence that landscape lowering within the Namche Barwa–Gyala Peri massif is coupled to river incision, much as has been suggested for the Nanga Parbat massif in the western Himalayan syntaxis (Burbank et al., 1996). Additionally, the similarity between patterns of relief—a good proxy for basin averaged erosion rates (Fig. 4)—and patterns of river incision potential further supports the interpretation that hillslopes and tributary catchments are slaved to the incision of the mainstem Yarlung Tsangpo–Brahmaputra and the Po Tsangpo. Finally, the conforming patterns of the current topography and of mineral cooling as recorded in both $^{40}Ar/^{39}Ar$ in biotite and (U-Th)/He in zircon indicate that the high erosion rates expressed by the current topography and fluvial geomorphology have been sustained for at least 1 m.y. (the age of the youngest $^{40}Ar/^{39}Ar$ age) and probably longer.

We emphasize that without being directly coupled to hillslope erosion, river incision alone,

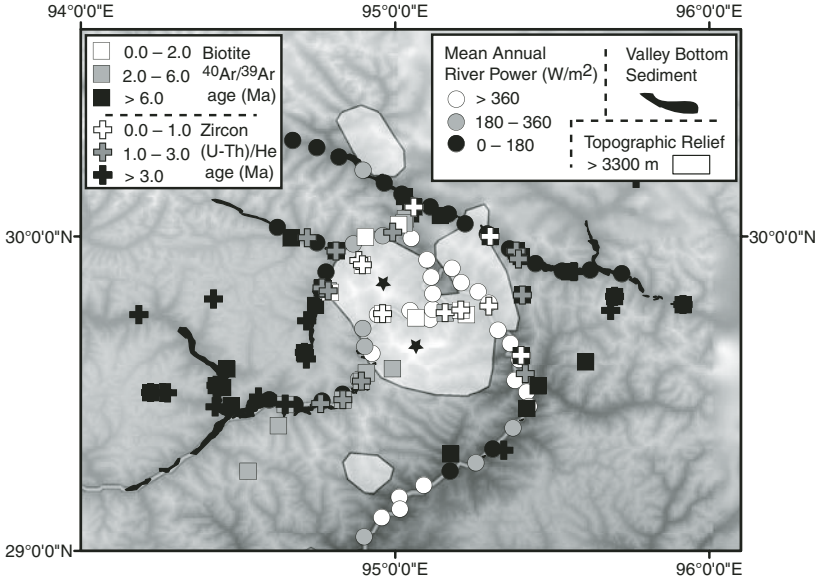

Figure 10. Superimposed patterns in topographic relief, sediment deposition, river power, zircon ages, and biotite ages. Stars denote the locations of Namche Barwa and Gyala Peri.

because of its relatively limited spatial area, would be insufficient to influence mass fluxes within an active orogen, as what we suggest is occurring within the Namche Barwa–Gyala Peri massif. The erosion of hillslopes and tributary channels must therefore be slaved to the incision of valley bottoms for river incision to drive rock uplift over a wide area (e.g., Burbank et al., 1996). The alternative, that in effect the incision of the Yarlung Tsangpo gorge reflects a transient wave of incision propagating into Tibet, is unlikely for three reasons. First, given the tens of kilometers of exhumation within the Namche Barwa–Gyala Peri massif since the Pliocene (Burg et al., 1997; Booth et al., 2004; Booth et al., 2007), it is essentially impossible for the young mineral ages in valley bottoms to reflect cooling owing to recent incision of only a 5-km-deep valley. Second, bedrock mapping in the syntaxis indicates that peaks are structurally continuous with rapidly cooled and deeply exhumed rocks in the gorge (Burg et al., 1997), suggesting that deep exhumation is continuous across peaks and valleys. Third, if the very young cooling ages in valley bottoms have been set simply by headward cutting of the Yarlung Tsangpo–Brahmaputra into Tibet, we anticipate that downstream of the knickpoint's current location there would be a trail of young cooling ages, corresponding to the former location of the propagating knickpoint. This scenario, however, is inconsistent with the older cooling ages present downstream of the knickpoint (Fig. 11). These arguments, taken together with the observations of the extremely steep slopes and active bedrock landsliding within the Yarlung Tsangpo gorge, lead us to conclude that the Yarlung Tsangpo–Brahmaputra River is driving regional denudation within the Namche Barwa–Gyala Peri massif.

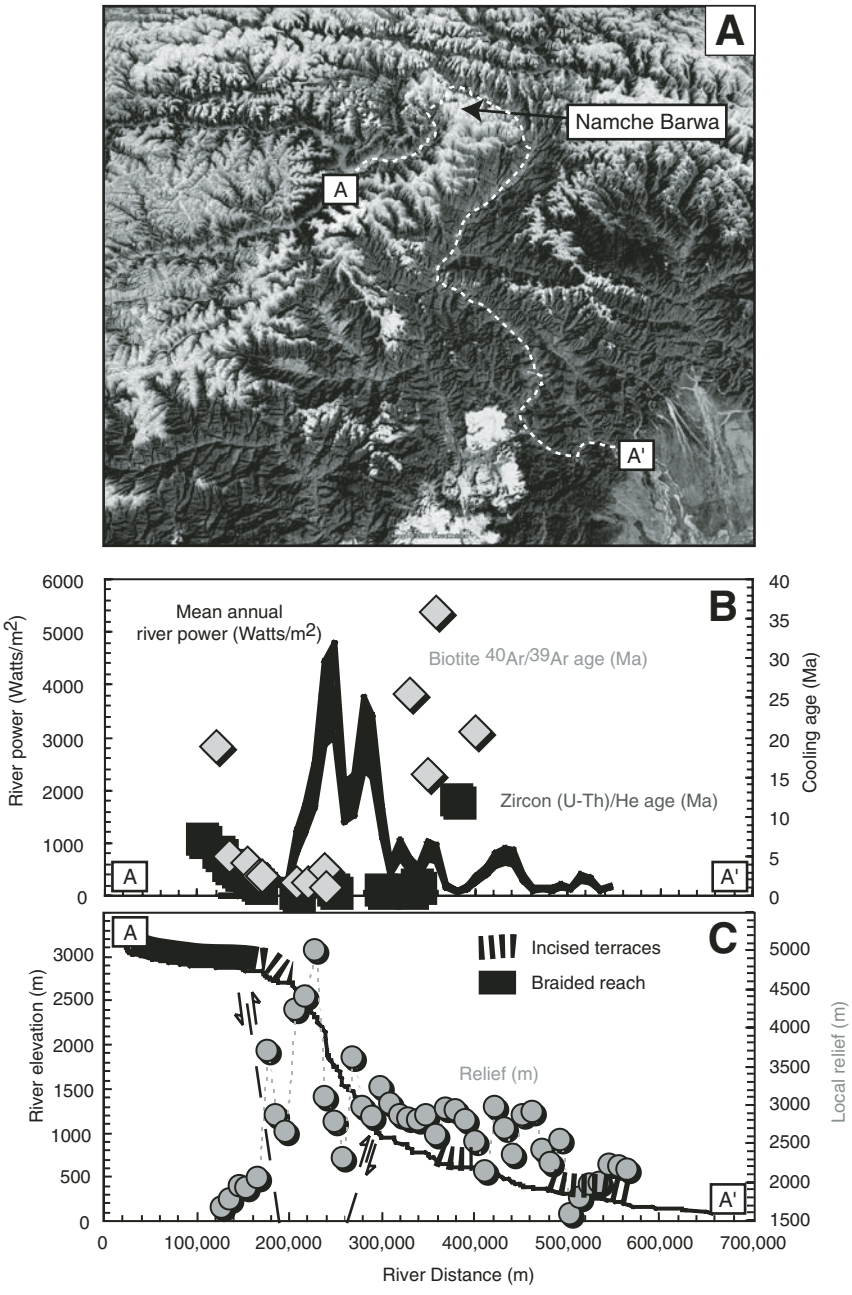

Figure 11. (A) Perspective satellite view of the study area, showing the reach of the Yarlung Tsangpo–Brahmaputra (A–A′) within the study area. (B) Longitudinal profile of zircon (U-Th)/He ages, biotite $^{40}Ar/^{39}Ar$ ages, and river power along the Yarlung Tsangpo–Brahmaputra. Uncertainty in river power is shown with line thickness, whereas error bars for mineral-cooling age data are smaller than the data symbols. (C) River elevation, topographic relief, and sediment storage along the Yarlung Tsangpo–Brahmaputra.

Because Namche Barwa and Gyala Peri are currently glaciated (Fig. DR2; see footnote 1), and were much more glaciated in the recent past (Montgomery et al., 2004), it is also natural to consider the role of glaciation in the exhumation of the Namche Barwa–Gyala Peri massif. Although we cannot rule out the possibility that glacial erosion, rather than fluvial erosion, is driving exhumation within the Namche Barwa–Gyala Peri massif, we offer several observations that point to fluvial erosion as the key process driving regional denudation. First, what sets the Namche Barwa–Gyala Peri massif apart from other high Himalayan peaks is not its steepness or ice volume, but instead its close spatial association with the largest and most powerful river in the Himalaya (Finlayson et al., 2002). Hence, to explain close coupling between glacial erosion and rock uplift here, we would have to provide an explanation for the reason why glacial erosion rates in this region would be unusually high. Neither the ice volumes, precipitation, nor hillslope angles are particularly remarkable by Himalayan standards, so we find no immediate suggestion for why glacial erosion would be higher here than elsewhere in the Himalaya, as is the case for river incision. Moreover, based on field observations (Fig. DR2; see footnote 1), it appears that large and potentially erosive valley glaciers did not extend into the region of rapid cooling outlined in Figures 2 and 3. Additionally, in the lower Yarlung Tsangpo gorge and

along the Po Tsangpo, we compute high river power and note young mineral-cooling ages, but the landscape in these regions is far from the influence of active glaciers, and the low channel elevations (<2300 m) and the lack of obvious glacial deposits in these regions make Quaternary glaciation unlikely. Hence, without any signs of active or past glacial erosion over much of the "bull's-eye" of rapid cooling shown in Figures 2 and 3, it is hard to invoke glacial erosion as the chief erosive agent in the study area.

Finally, we note that although glacial erosion itself may not be the primary driver of exhumation within the Namche Barwa–Gyala Peri massif, the damming of the Yarlung Tsangpo–Brahmaputra by glacial advances likely unleashed repeated catastrophic glacial dam-break floods down the Yarlung Tsangpo gorge over the Quaternary (Montgomery et al., 2004). These floods may have been essential for the rapid incision of the Yarlung Tsangpo gorge over the Quaternary. However, without more detailed glacial and glacial lake chronologies in the region, the importance of these events, and by extension glaciation, on the landscape evolution of the Namche Barwa–Gyala Peri massif remains uncertain.

Exhumation of the Namche Barwa–Gyala Peri massif is also unlikely to be related to crustal extension, which is often invoked as the exhumational mechanism for isolated metamorphic massifs. Where extensional faulting is responsible for unroofing deep crustal rocks, there is no reason to expect a close correspondence between erosion and exhumation, because faulting itself is the primary mechanism of mass removal above a core complex. Additionally, the thrust motion along faults bounding the Namche Barwa–Gyala Peri massif (Burg et al., 1998; Kidd et al., 2006) and the structural fabric mapped in detail by Burg et al. (1998) are both inconsistent with extensional exhumation.

Prior studies have recognized the importance of the Yarlung Tsangpo–Brahmaputra to the geodynamics of the syntaxis (Burg et al., 1998; Zeitler et al., 2001b; Koons et al., 2002). Zeitler et al. (2001b) and Koons et al. (2002) attribute uplift of the Namche Barwa–Gyala Peri massif directly to the influence of regional denudation driven by river incision via the tectonic aneurysm hypothesis. In contrast, Burg et al. (1998) suggest that the Yarlung Tsangpo–Brahmaputra and its tributaries, although vital to the exhumation of the massif, are nevertheless antecedent to what is fundamentally a lithospheric buckling instability. It is challenging to distinguish between these end-member models for the tectonic development of the Namche Barwa–Gyala Peri massif, because both require a close correspondence between surface erosion and rock uplift. However, a number of features of the region discussed below are well explained by dynamic coupling between denudation driven by river incision and rock uplift.

From the perspective of a buckle fold origin for the Namche Barwa–Gyala Peri massif (Burg et al., 1998), the patterns of relief, river morphology, and cooling ages shown in Figure 10 would require a fortuitous coincidence of the location of maximum buckle folding and the location of the Yarlung Tsangpo–Brahmaputra knickpoint. As noted earlier, high topographic relief is closely associated with rapid rock uplift inferred from GPS and seismicity (Bendick and Bilham, 2001) along the Main Himalayan Thrust. However, whereas high relief forms a more or less continuous band along the Himalayan front in response to uplift along the Main Himalayan Thrust, in the core of the eastern syntaxis high relief, rapid cooling, and by inference rock uplift are extremely localized within a region of rapid inferred river incision. Given the apparently highly localized nature of rapid rock uplift within the Namche Barwa–Gyala Peri massif, it is therefore striking that the steepest portion of the Yarlung Tsangpo–Brahmpatura, the largest river in the Himalaya and Tibet, is centered precisely on the Namche Barwa–Gyala Peri uplift. This is particularly notable because rivers tend to be deflected around actively uplifting antiforms (e.g., van der Beek et al., 2002) rather than incorporated within their structural or topographic culminations—that is, unless the rivers themselves are responsible for the location of the structure (e.g., Oberlander, 1985; Zeitler et al., 2001b; Koons et al., 2002; Simpson, 2004; Montgomery and Stolar, 2006).

A longitudinal perspective of the river reveals that the great knickpoint of the Yarlung Tsangpo–Brahmaputra and its zone of rapid inferred incision rates are centered directly on the region of rapid zircon and biotite cooling, as well as on the zone of extreme local relief (Fig. 11). In the absence of tectonic uplift, the rate of knickpoint propagation upstream for an orogen-traversing river such as the Yarlung Tsangpo–Brahmaputra can be estimated via equation 14 in Lavé and Avouac (2001), a model for the erosive propagation of a steep river reach into a mountain front:

$$m(x,t) = S(x)^{-1}(1 - \rho_c/\rho_m)i(x,t), \qquad (2)$$

where m is the knickpoint propagation rate upstream, $i(x,t)$ is the vertical incision rate of the knickpoint, S is channel slope, and ρ_c and ρ_m are the density of the crust and mantle, respectively. As noted by Lavé and Avouac (2001), because equation 2 assumes local isostatic compensation, it provides a conservative estimate of knickpoint propagation rates in most settings. Nevertheless, assuming a reasonable range of incision rates between 1 and 10 mm/yr, the ~2% gradient Yarlung Tsangpo–Brahmaputra knickpoint would, according to equation 2, propagate upstream at a minimum rate of between 30 and 300 km/m.y. The fact that high inferred river incision rates and young zircon and biotite cooling ages are all spatially colocated along the Yarlung Tsangpo–Brahmaputra, however, indicates that the location of rapid incision has not propagated upstream. Otherwise we would observe a mismatch between the location of current rapid incision and the location of rapid exhumation in the past, as revealed by the cooling age data. Thus we infer that the Yarlung Tsangpo–Brahmaputra knickpoint has been pinned by the uplift of the Namche Barwa–Gyala Peri massif—an inference also supported by the localization of high relief within the zone of rapid cooling and high inferred incision rates (Fig. 11). Without compensatory uplift of the Namche Barwa–Gyala Peri massif, the Yarlung Tsangpo–Brahmaputra knickpoint would have propagated well into Tibet.

In considering the coincidence of the Yarlung Tsangpo gorge and the Namche Barwa–Gyala Peri massif, one might ask how what is widely regarded as the most erosive river in the Himalaya (Finlayson et al., 2002) became superimposed on the one structure apparently capable of balancing its incision? As noted previously, Koons et al. (2002) argue that isolated, active, high-relief metamorphic massifs spatially colocated with large and erosive rivers is an expected consequence of erosional, thermal, and mechanical coupling in an active orogen. Hence, the colocation of the Namche Barwa–Gyala Peri massif and the Yarlung Tsangpo gorge is not likely to be a coincidence but instead probably emerges from the strong coupling between denudation driven by river incision, deformation, and rock uplift within this region of the Himalaya.

Inferring Long-Term River Incision Rates from Fluvial Geomorphology

Prior field studies investigating evidence for coupling between rock uplift, surface erosion, and fluvial geomorphology have focused on the relationship of several fluvial geomorphic indices of incision rate to a variety of exhumation rate data (e.g., Burbank et al., 1996; Burbank et al., 2003; Wobus et al., 2003; Vannay et al., 2004; Mitchell and Montgomery, 2006; Wobus et al., 2006). Burbank et al. (1996), Wobus et al. (2003), and Vannay et al. (2004) report spatial correlations of river steepness and muscovite mineral cooling ages in the western Himalaya, central Nepal Himalaya, and Sutlej Valley, India. In contrast, Mitchell and Montgomery (2006) and Burbank et al. (2003), respectively,

illustrate that trends in river power are not well correlated with those in apatite ages from the western Cascades of Washington State, and from the central Nepal Himalaya. Additionally, Tomkin et al. (2003) show that apart from even agreeing with cooling ages, patterns in river power also are not correlative with incision rates in the Olympic Mountains of Washington State. All of this suggests that inferring long-term incision rates strictly from fluvial geomorphology is an imperfect art at best and that factors such as sediment supply (e.g., Brandon and Gasparini, 2005) or the glacial legacy of a mountainous landscape (Mitchell and Montgomery, 2006) may confound attempts to infer long-term incision rates solely on the basis of present-day channel morphology.

Acknowledging these complications, we have presented two separate methods for inferring patterns in rates of river incision throughout the study area. Despite the potentially complicating effects of sediment supply and cover on estimating rates of river incision (Sklar and Dietrich, 2004; Brandon and Gasparini, 2005), in the vicinity of the Namche Barwa–Gyala Peri massif there is a strong correspondence of incision rates inferred from only river power patterns and those inferred from taking sediment dynamics more directly into account. More significantly, both of these indices of river incision also provide reasonably accurate and complementary pictures of the spatial patterns in long-term erosion-rate gradients inferred from mineral-cooling data.

Thus despite numerous reasons for why a snapshot of river morphology should reveal little about the long-term erosion of a landscape, river-power patterns and sediment-deposition patterns nevertheless appear to conform to exhumation gradients within the study area. This in turn underscores the fact that present-day gradients in exhumation across the Namche Barwa–Gyala Peri massif have been sustained over the recent geologic past, and that in the absence of mineral-cooling data, fluvial geomorphology can provide an important proxy for patterns in exhumation in studies of active tectonics, as has been suggested by others (e.g., Finlayson et al., 2002; Wobus et al., 2003, 2006).

Precipitation and Exhumation

As discussed in the introduction, a virtue of our study area is that we are able to compare patterns in precipitation and patterns in river power independently with patterns in mineral-cooling ages. This is possible in the vicinity of the Namche Barwa–Gyala Peri massif because the addition of locally derived orographic precipitation to the Yarlung Tsangpo gorge accounts for only ~10% of the combined discharge of the Po Tsangpo and Yarlung Tsangpo–Brahmaputra, which together drain ~200,000 km^2 of the Tibetan Plateau. Hence, precipitation and river power on the Yarlung Tsangpo–Brahmaputra River are effectively decoupled and can each be compared to exhumation rate patterns to assess the relative strengths of these two forcings on patterns of mineral-cooling ages.

Although patterns in orographic precipitation have been found to control patterns in exhumation of the Himayalan front (Thiede et al., 2005) and the Washington Cascades (Reiners et al., 2003), there is no clear spatial relationship within the Namche Barwa–Gyala Peri massif between patterns in precipitation and cooling ages (Fig. 12), as there is for patterns in river power and cooling ages (Fig. 11). We interpret this as evidence that within the study area, hillslope erosion rates are much more closely coupled to local-channel incision rates (and therefore local base level) than they are to local precipitation totals and the processes that depend on them. Otherwise, we would anticipate a closer relationship between exhumation patterns and precipitation patterns.

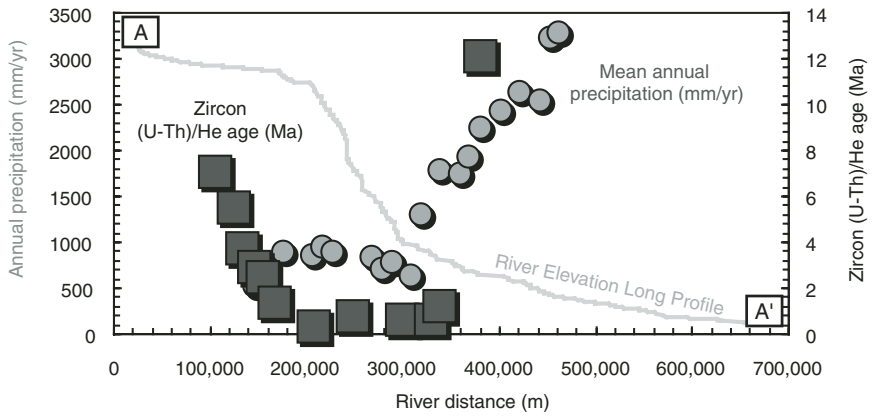

Figure 12. Profiles of elevation, precipitation, and zircon (U-Th)/He ages along the Yarlung Tsangpo–Brahmaputra.

CONCLUSIONS

We have compared spatial patterns in inferred detachment-limited incision rates and saltation-abrasion potential to patterns in topographic relief, precipitation, and exhumation rates reflected by zircon- and biotite-cooling ages in the vicinity of the Namche Barwa–Gyala Peri massif. Mapping indicates a spatial colocation of high incision-rate potential, sediment-transport efficiency, relief, and mineral-cooling rates focused on this massif. Only patterns in precipitation appear uncorrelated with those in mineral-cooling ages, suggesting that it is not directly tied to exhumation within the Namche Barwa–Gyala Peri massif. Taken together, these observations suggest strongly that regional denudation driven by river incision, combined with efficient sediment evacuation within the region of the Yarlung Tsangpo gorge, is closely coupled with vertical rock uplift.

Isolated, active, high-relief metamorphic massifs spatially colocated with large and erosive rivers are an expected consequence of erosional and thermo-mechanical coupling in an active orogen (Koons et al., 2002). A number of key features of the Namche Barwa–Gyala Peri massif suggest that the Yarlung Tsangpo–Brahmaputra River plays a significant role in controlling lithospheric dynamics here: (1) Along much of the Himalaya front, areas of high relief and young cooling ages form a continuous band related to active rock uplift along the Main Himalayan Thrust. However, high relief and rapid mineral cooling in the vicinity of the Namche Barwa–Gyala Peri massif is restricted to a "bull's-eye" pattern precisely in the region cut by the largest river in the Himalaya, the Yarlung Tsangpo–Brahmaputra, suggesting that rock uplift is equally localized. (2) The coincidence of high river power, high relief, and the patterns in young zircon- and biotite-cooling ages requires that the location of rapid incision on the Yarlung Tsangpo–Brahmaputra be pinned for at least 1 m.y. Without a close balance between the uplift of the Namche Barwa–Gyala Peri massif and the incision of the Yarlung Tsangpo–Brahmaputra knickpoint, a wave of headward incision would have propagated rapidly into Tibet. Within its deep gorge, the Yarlung Tsangpo–Brahmaputra is the most powerful reach of river in the Himalaya. It is therefore striking that it is colocated with the one structure that is apparently capable of balancing its incision.

ACKNOWLEDGMENTS

Funding was provided by the Continental Dynamics Program of the U.S. National Science Foundation (EAR-0003561 to B.H., D.R.M., and J.O.S., and EAR-0003462 to P.K.Z.) and a National Science Foundation Graduate Research Fellowship to N.J.F. We thank Douglas Burbank, Lewis Owen, and an anonymous reviewer for clear and constructive reviews. We also thank Peter Koons and Bill Kidd for numerous discussions about the tectonics and geodynamics of eastern Tibet, and Bill Kidd for generously providing the geologic map of the study area.

REFERENCES CITED

Anders, A.M., 2005, The co-evolution of precipitation and topography [Ph.D. thesis]: Seattle, University of Washington, 248 p.

Anders, A.M., Roe, G.H., Hallet, B., Montgomery, D.R., Finnegan, N.J., and Putkonen, J., 2006, Spatial patterns of precipitation and topography in the Himalaya, *in* Willett, S.D., et al., eds., Tectonics, climate, and landscape evolution: Geological Society of America Special Paper 398, p. 39–53.

Armijo, R., Tapponnier, P., and Han, Tonglin, 1989, Late Cenozoic right-lateral strike-slip faulting across southern Tibet: Journal of Geophysical Research, v. 94, p. 2787–2838.

Beaumont, C., Jamieson, R.A., Nguyen, M.H., and Lee, B., 2001, Himalayan tectonics explained by extrusion of a low-viscosity crustal channel coupled to focused surface denudation: Nature, v. 414, p. 738–742, doi: 10.1038/414738a.

Bendick, R., and Bilham, R., 2001, How perfect is the Himalayan arc?: Geology, v. 29, p. 791–794, doi: 10.1130/0091-7613(2001)029<0791:HPITHA>2.0.CO;2.

Booth, A.L., Zeitler, P.K., Kidd, W.S.F., Wooden, J., Liu, Y., Idleman, B., Hren, M., and Chamberlain, C.P., 2004, U-Pb zircon constraints on the tectonic evolution of southeastern Tibet, Namche Barwa Area: American Journal of Science, v. 304, p. 889–929, doi: 10.2475/ajs.304.10.889.

Booth, A.L., Chamberlain, C.P., Kidd, W.S.F., and Zeitler, P.K., 2007, Metamorphic and geochronologic constraints on the tectonic evolution of the eastern Himalayan syntaxis: Namche Barwa: Geological Society of America Bulletin.

Brandon, M.T., and Gasparini, N.M., 2005, A power-law approximation for fluvial incision by tools and bed-coverage processes: Eos (Transactions, American Geophysical Union), v. 86, Abstract H53D–0515.

Brookfield, M.E., 1998, The evolution of the great river systems of southern Asia during the Cenozoic India-Asia collision: Rivers draining southwards: Geomorphology, v. 22, p. 285–312, doi: 10.1016/S0169-555X(97)00082-2.

Bunn, J.T., Finnegan, N.J., and Montgomery, D.R., 2004, Landsliding and stream power in the vicinity of the Tsangpo River gorge at Namche Barwa, eastern Tibet: Geological Society of America Abstracts with Programs, v. 36, no. 4, p. 33.

Burbank, D.W., Leland, J., Fielding, E., Anderson, R.S., Brozovic, N., Reid, M.R., and Duncan, C., 1996, Bedrock incision, rock uplift and threshold hillslopes in the northwestern Himalayas: Nature, v. 379, p. 505–510, doi: 10.1038/379505a0.

Burbank, D.W., Blythe, A.E., Putkonen, J., Pratt-Sitaula, B., Gabet, E., Oskin, M., Barros, A., and Ojha, T.P., 2003, Decoupling of erosion and precipitation in the Himalayas: Nature, v. 426, p. 652–655, doi: 10.1038/nature02187.

Burg, J.P., Davy, P., Nievergelt, P., Oberli, F., Seward, D., Diao, Z., and Meier, M., 1997, Exhumation during crustal folding in the Namche Barwa syntaxis: Terra Nova, v. 9, p. 53–56, doi: 10.1111/j.1365-3121.1997.tb00001.x.

Burg, J.P., Nievergelt, P., Oberli, F., Seward, D., Davy, P., Maurin, J.C., Diao, Z., and Meier, M., 1998, The Namche Barwa syntaxis; evidence for exhumation related to compressional crustal folding: Journal of Asian Earth Sciences, v. 16, p. 239–252, doi: 10.1016/S0743-9547(98)00002-6.

Clark, M.K., Schoenbohm, L.M., Royden, L.H., Whipple, K.X., Burchfiel, B.C., Zhang, X., Tang, W., Wang, E., and Chen, L., 2004, Surface uplift, tectonics, and erosion of eastern Tibet from large-scale drainage patterns: Tectonics, v. 23, p. TC1006, doi: 10.1029/2002TC001402.

Ding, L., Zhong, D., Yin, A., Kapp, P., and Harrison, T.M., 2001, Cenozoic structural and metamorphic evolution of the eastern Himalayan syntaxis (Namche Barwa): Earth and Planetary Science Letters, v. 192, p. 423–438, doi: 10.1016/S0012-821X(01)00463-0.

Finlayson, D.P., Montgomery, D.R., and Hallet, B., 2002, Spatial coincidence of rapid inferred erosion with young metamorphic massifs in the Himalayas: Geology, v. 30, p. 219–222, doi: 10.1130/0091-7613(2002)030<0219:SCORIE>2.0.CO;2.

Finnegan, N.J., Roe, G.H., Montgomery, D.R., and Hallet, B., 2005, Controls on the channel width of rivers: Implications for modeling fluvial incision of bedrock: Geology, v. 33, p. 229–232, doi: 10.1130/G21171.1.

Finnegan, N.J., Sklar, L.S., and Fuller, T.K., 2007, Interplay of sediment supply, river incision, and channel morphology revealed by the transient evolution of an experimental bedrock channel: Journal of Geophysical Research, v. 112, p. F03S11, doi:10.1029/2006JF000569.

Gilbert, G.K., 1877, Report on the Geology of the Henry Mountains: Washington, D.C., U.S. Government Printing Office, 160 p.

Grove, M., and Harrison, M.T., 1996, ^{40}Ar diffusion in Fe-rich biotite: American Mineralogist, v. 81, p. 940–951.

Hallet, B., and Molnar, P., 2001, Distorted drainage basins as markers of crustal strain east of the Himalaya: Journal of Geophysical Research, v. 106, p. 13,697–13,709, doi: 10.1029/2000JB900335.

Hodges, K.V., 2000, Tectonics of the Himalaya and southern Tibet from two perspectives: Geological Society of America Bulletin, v. 112, p. 324–350, doi: 10.1130/0016-7606(2000)112<0324:TOTHAS>2.3.CO;2.

Howard, A.D., 1994, A detachment-limited model of drainage basin evolution: Water Resources Research, v. 30, p. 2261–2285, doi: 10.1029/94WR00757.

Kidd, W.S., Lim, C., Zeitler, P.K., Enkelmann, E., Booth, A.L., Chamberlain, C.P., Tang, W., Liu, Y., and Craw, D., 2006, Structural and tectonic geology of the Namche Barwa–Gyala Peri antiform, southeastern Tibet: Eos (Transactions, American Geophysical Union), v. 87, Abstract T23-0480.

Kirby, E., and Whipple, K.X., 2001, Quantifying differential rock-uplift rates via stream profile analysis: Geology, v. 29, p. 415–418, doi: 10.1130/0091-7613(2001)029<0415:QDRURV>2.0.CO;2.

Kirby, E., Whipple, K.X., Tang, W., and Chen, Z., 2003, Distribution of active rock uplift along the eastern margin of the Tibetan Plateau: Inferences from bedrock channel longitudinal profiles: Journal of Geophysical Research, v. 108, p. 2217, doi: 10.1029/2001JB000861.

Koons, P.O., 1995, Modeling the topographic evolution of collisional belts: Annual Review of Earth and Planetary Sciences, v. 23, p. 375–408, doi: 10.1146/annurev.ea.23.050195.002111.

Koons, P.O., Zeitler, P.K., Chamberlain, C.P., Craw, D., and Meltzer, A.S., 2002, Mechanical links between erosion and metamorphism in Nanga Parbat, Pakistan Himalaya: American Journal of Science, v. 302, p. 749–773, doi: 10.2475/ajs.302.9.749.

Lavé, J., and Avouac, J.P., 2001, Fluvial incision and tectonic uplift across the Himalayas of central Nepal: Journal of Geophysical Research, v. 106, p. 26,561–26,592, doi: 10.1029/2001JB000359.

Malloy, M., 2004, Rapid erosion at the Tsangpo knickpoint and exhumation of southeastern Tibet [M.S. thesis]: Bethlehem, Pennsylvania, Lehigh University, 84 p.

Meltzer, A.S., Sarker, G.L., Seeber, L., and Armbruster, J., 1998, Snap, crackle, pop!: Seismicity and crustal structure at Nanga Parbat, Pakistan, Himalaya: Eos (Transactions, American Geophysical Union), v. 79, Abstract T41E–06.

Mitchell, S.G., and Montgomery, D.R., 2006, Influence of a glacial buzzsaw on the height and morphology of the central Washington Cascade Range, USA: Quaternary Research, v. 65, p. 96–107, doi: 10.1016/j.yqres.2005.08.018.

Molnar, P., Anderson, R.S., Kier, G., and Rose, J., 2006, Relationships among probability distributions of stream discharges in floods, climate, bed load transport, and river incision: Journal of Geophysical Research, v. 111, doi: 10.1029/2005JF000310.

Montgomery, D.R., and Brandon, M.T., 2002, Topographic controls on erosion rates in tectonically active mountain ranges: Earth and Planetary Science Letters, v. 201, p. 481–489, doi: 10.1016/S0012-821X(02)00725-2.

Montgomery, D.R., and Gran, K.B., 2001, Downstream variations in the width of bedrock channels: Water Resources Research, v. 37, doi: 10.1029/2000WR900393.

Montgomery, D.R., and Stolar, D.B., 2006, Reconsidering Himalayan river anticlines: Geomorphology, v. 82, p. 4–15, doi: 10.1016/j.geomorph.2005.08.021.

Montgomery, D.R., Hallet, B., Yuping, L., Finnegan, N., Anders, A., and Gillespie, A., 2004, Evidence for Holocene megafloods down the Tsangpo River gorge: Southeastern Tibet: Quaternary Research, v. 62, p. 201–207, doi: 10.1016/j.yqres.2004.06.008.

Niemi, N.A., Oskin, M., Burbank, D.W., Heimsath, A.M., and Gabet, E.J., 2005, Effects of bedrock landslides on cosmogenically determined erosion rates: Earth and Planetary Science Letters, v. 237, p. 480–498, doi: 10.1016/j.epsl.2005.07.009.

Oberlander, T.M., 1985, Origin of drainage transverse to structures in orogens, *in* Morisawa, M., and Hack, J.T., eds., Tectonic geomorphology: Boston, Allen and Unwin, p. 155–182.

Park, S., and Mackie, R., 2000, Resistive (dry?) lower crust in an active orogen, Nanga Parbat, northern Pakistan: Tectonophysics, v. 316, p. 359–380, doi: 10.1016/S0040-1951(99)00264-4.

Reiners, P.W., Farley, K.A., and Hickes, H.J., 2002, He diffusion and (U–Th)/He thermochronometry of zircon: Initial results from Fish Canyon Tuff and Gold Butte: Tectonophysics, v. 349, p. 297–308, doi: 10.1016/S0040-1951(02)00058-6.

Reiners, P., Ehlers, T., Mitchell, S., and Montgomery, D., 2003, Coupled spatial variations in precipitation and long-term erosion rates across the Washington Cascades: Nature, v. 426, p. 645–647, doi: 10.1038/nature02111.

Roe, G.H., Montgomery, D.R., and Hallet, B., 2002, Effects of orographic precipitation variations on the concavity of steady-state river profiles: Geology, v. 30, p. 143–146, doi: 10.1130/0091-7613(2002)030<0143:EOOPVO>2.0.CO;2.

Roe, G.H., Stolar, D.B., and Willett, S.D., 2006, Response of a steady-state critical wedge orogen to changes in climate and tectonic forcing, *in* Willett, S.D., et al., eds., Tectonics, climate, and landscape evolution: Geological Society of America Special Paper 398, p. 227–239.

Royden, L.H., Burchfiel, B.C., King, R.W., Wang, E., Chen, Z., Shen, F., and Liu, Y., 1997, Surface deformation and lower crustal flow in eastern Tibet: Science, v. 276, p. 788–790, doi: 10.1126/science.276.5313.788.

Seeber, L., and Gornitz, V., 1983, River profiles along the Himalayan Arc as indicators of active tectonics: Tectonophysics, v. 92, p. 335–367, doi: 10.1016/0040-1951(83)90201-9.

Simpson, G., 2004, Role of river incision in enhancing deformation: Geology, v. 32, p. 341–344, doi: 10.1130/G20190.2.

Sklar, L. and Dietrich, W.E., 1998, River longitudinal profiles and bedrock incision models: Stream power and the influence of sediment supply, *in* Tinkler, K.J., and, Wohl, E.E., eds., Rivers over rock: Fluvial processes in bedrock channels, American Geophysical Union Geophysical Monograph, v. 107, p. 237-260.

Sklar, L.S., and Dietrich, W.E., 2001, Sediment and rock strength controls on river incision into bedrock: Geology, v. 29, p. 1087–1090, doi: 10.1130/0091-7613(2001)029<1087:SARSCO>2.0.CO;2.

Sklar, L.S., and Dietrich, W.E., 2004, A mechanistic model for river incision into bedrock by saltating bed load: Water Resources Research, v. 40, p. W06301, doi: 10.1029/2003WR002496.

Sol, S., Meltzer, A., Bürgmann, R., van der Hilst, R.D., King, R., Chen, Z., Koons, P.O., Lev, E., Liu, Y.P., Zeitler, P.K., Zhang, X., Zhang, J., and Zurek, B., 2007, Geodynamics of the southeastern Tibetan Plateau from seismic anisotropy and geodesy: Geology, v. 35, p. 563–566, doi: 10.1130/G23408A.1.

Stock, J.D., and Montgomery, D.R., 1999, Geologic constraints on bedrock river incision using the stream power law: Journal of Geophysical Research, v. 104, p. 4983–4993, doi: 10.1029/98JB02139.

Stolar, D.B., Willett, S.D., and Roe, G.H., 2006, Climatic and tectonic forcing of a critical orogen, *in* Willett, S.D., et al., eds., Tectonics, climate, and landscape evolution: Geological Society of America Special Paper 398, p. 241–250.

Stuwe, K., White, L., and Brown, R., 1994, The influence of eroding topography on steady-state isotherms; application to fission track analysis: Earth and Planetary Science Letters, v. 124, p. 63–74, doi: 10.1016/0012–821X (94)00068–9.

Tapponnier, R., Peltzer, G., Le Dain, A.Y., Armijo, R., and Cobbold, P., 1982, Propagating extrusion tectonics in Asia; new insights from simple experiments with plasticine: Geology, v. 10, p. 611–616, doi: 10.1130/0091-7613(1982)10<611:PETIAN>2.0.CO;2.

Thiede, R.C., Arrowsmith, J.R., Bookhagen, B., McWilliams, M.O., Sobel, E.R., and Strecker, M.R., 2005, From tectonically to erosionally controlled development of the Himalayan orogen: Geology, v. 33, p. 689–692, doi: 10.1130/G21483.1.

Tomkin, J.H., Brandon, M.T., Pazzaglia, F.J., Barbour, J.R., and Willett, S.D., 2003, Quantitative testing of bedrock incision models for the Clearwater River, NW Washington State: Journal of Geophysical Research, B, Solid Earth and Planets, v. 108, doi: 10.1029/2002JB002087.

U.S. Geological Survey, 1993, Digital elevation models, Data user guide 5: Reston, Virginia, 50 p.

Vance, D., Bickle, M., Ivy-Ochs, S., and Kubik, P.W., 2003, Erosion and exhumation in the Himalaya from cosmogenic isotope inventories of river sediments: Earth and Planetary Science Letters, v. 206, p. 273–288, doi: 10.1016/S0012-821X(02)01102-0.

van der Beek, P., Champel, B., and Mugnier, J.-L., 2002, Control of detachment dip on drainage development in regions of active fault-propagation folding: Geology, v. 30, p. 471–474, doi: 10.1130/0091-7613(2002)030<0471:CODDOD>2.0.CO;2.

Vannay, J.C., Grasemann, B., Rahn, M., Frank, W., Carter, A., and Baudraz, V., 2004, Miocene to Holocene exhumation of metamorphic crustal wedges in the Himalayan orogen: Evidence for tectonic extrusion coupled to fluvial erosion: Tectonics, v. 23, doi: 10.1029/2002TC001429.

Whipple, K.X., and Meade, B.J., 2004, Controls on the strength of coupling among climate, erosion, and deformation in two-sided, frictional orogenic wedges at steady state: Journal of Geophysical Research, v. 109, p. F01011, doi: 10.1029/2003JF000019.

Whipple, K.X., and Tucker, G.E., 1999, Dynamics of the stream-power river incision model: Implications for height limits of mountain ranges, landscape response timescales, and research needs: Journal of Geophysical Research, B, Solid Earth and Planets, v. 104, p. 17,661–17,674, doi: 10.1029/1999JB900120.

Whipple KX, Hancock GS, Anderson RS, 2000, River incision into bedrock: Mechanics and relative efficacy of plucking, abrasion, and cavitation: Geological Society of America Bulletin, v. 112, p. 490–503.

Whittaker, A.C., Cowie, P.A., Attal, M., Tucker, G.E., and Roberts, G.P., 2007, Bedrock channel adjustment to tectonic forcing: Implications for predicting river incision rates: Geology, v. 35, p. 103–106, doi: 10.1130/G23106A.1.

Willett, S.D., 1999, Orogeny and orography: The effects of erosion on the structure of mountain belts: Journal of Geophysical Research, v. 104, p. 28,957–28,982, doi: 10.1029/1999JB900248.

Willett, S.D., Schlunegger, F., and Picotti, V., 2006, Messinian climate change and erosional destruction of the central European Alps: Geology, v. 34, p. 613–616, doi: 10.1130/G22280.1.

Wobus, C.W., Hodges, K.V., and Whipple, K.X., 2003, Has focused denudation sustained active thrusting at the Himalayan topographic front?: Geology, v. 31, p. 861–864, doi: 10.1130/G19730.1.

Wobus, C.W., Whipple, K.X., and Hodges, K.V., 2006, Neotectonics of the central Nepalese Himalaya: Constraints from geomorphology, detrital $^{40}Ar/^{39}Ar$ thermochronometry, and thermal modeling: Tectonics, v. 25, doi: 10.1029/2005TC001935.

Zeitler, P.K., Chamberlain, C.P., and Smith, H.A., 1993, Synchronous anatexis, metamorphism, and rapid denudation at Nanga Parbat, Pakistan Himalaya: Geology, v. 21, p. 347–350, doi: 10.1130/0091-7613(1993)021<0347:SAMARD>2.3.CO;2.

Zeitler, P.K., Koons, P.O., Bishop, M.L., Chamberlain, C.P., Craw, D., Edwards, M.A., Hamidullah, S., Jan, M.Q., Khan, M.A., Khattak, M.U.K., Kidd, W.S.F., Mackie, R.L., Meltzer, A.S., Park, S.K., Pecher, A., Poage, M.A., Sarker, G., Schneider, D.A., Seeber, L., and Shroder, J., 2001a, Crustal reworking at Nanga Parbat, Pakistan: Evidence for erosional focusing of crustal strain: Tectonics, v. 20, p. 712–728, doi: 10.1029/2000TC001243.

Zeitler, P.K., Meltzer, A.S., Koons, P.O., Craw, D., Hallet, B., Chamberlain, C.P., Kidd, W.S.F., Park, S.K., Seeber, L., Bishop, M., and Shroder, J., 2001b, Erosion, Himalayan geodynamics, and the geomorphology of metamorphism: GSA Today, v. 11, no. 1, p. 4–9, doi: 10.1130/1052-5173(2001)011<0004:EHGATG>2.0.CO;2.

Zeitler, P.K., Malloy, M.A., Kutney, M.P., Idleman, B.D., Liu, Y., Kidd, W.S., and Booth, A.L., 2006, Geochronological evidence for the tectonic and topographic evolution of SE Tibet: Eos (Transactions, American Geophysical Union), v. 87, Abstract T23B–0480.

Zhang, P.Z., Shen, Z., Wang, M., Gan, W., Bürgmann, R., Molnar, P., Wang, Q., Niu, Z., Sun, J., Wu, J., Hanrong, S., and Xinzhao, Y., 2004, Continuous deformation of the Tibetan Plateau from global positioning system data: Geology, v. 32, p. 809–812, doi: 10.1130/G20554.1.

Manuscript Received 13 March 2007
Revised Manuscript Received 3 September 2007
Manuscript Accepted 5 September 2007

Printed in the USA